DETERMINATION OF THE TEMPERATURE FIELD USING LIQUID CRYSTAL THERMOGRAPHY AND ANALYSIS OF TWO-PHASE FLOW STRUCTURES IN RESEARCH ON BOILING HEAT TRANSFER IN A MINICHANNEL

Magdalena Piasecka

Kielce University of Technology, Department of Mechanics, Al. 1000-lecia P.P. 7, 25-314 Kielce, Poland, (✉ tmpmj@tu.kielce.pl, +48 41 3424320)

Abstract

The paper presents the application of liquid crystal thermography for temperature determination and visualisation of two phase flow images on the studied surface. Properties and applications of thermochromic liquid crystals are discussed. Liquid crystals were applied for two-dimensional detection of the temperature of the heating foil forming one of the surfaces of the minichannel along which the cooling liquid flowed. The heat flux supplied to the heating surface was altered in the investigation and it was accompanied by a change in the color distribution on the surface. The accuracy of temperature measurements on the surface with liquid crystal thermography is estimated. The method of visualisation of two-phase flow structures is described. The analysis of monochrome images of flow structures was employed to calculate the void fraction for some cross-sections. The flow structure photos were processed using Corel graphics software and binarized. The analysis of phase volumes employed Techsystem Globe software. The measurement error of void fraction is estimated.

Keywords: temperature measurement, liquid crystal thermography, measurement accuracy, void fraction.

1. Introduction to application of liquid crystal thermography

1.1. Applications of liquid crystals

Liquid crystals have been widely applied in technology because of their unique properties manifested in the change of color and/or its intensity. That can be used to detect very slight changes in temperature, stress, electromagnetic radiation or chemical agent properties. At present, the most popular liquid crystal applications make use of the above-mentioned property of light-selective reflection from planar oriented layers of the substance. The color of the selectively reflected light depends on many external factors such as: mechanical action, white light incidence angle, etc. What is of particular importance in the field of heat transfer applications, is the color dependence on the temperature of the surface observed. Due to the above-mentioned properties of thermochromic liquid crystals, the layer covering the surface of a solid provides an accurate colorful mapping of temperature distribution on this surface. Such a means of indicating the temperature distribution is called *thermography*; it is one of the most precise and convenient methods of determining a two-dimensional temperature distribution on any surface. The temperature range in which particles of thermochromic liquid crystals reflect the visible spectrum is called the *active band*. At the beginning of thermographic investigations, it is necessary to select an appropriate liquid crystals mixture so that, at the lowest temperature on the given surface, the color of the selective reflection would be red and then, would change in the sequence of the visible spectrum (red, yellow, green,

blue, violet) into violet at the highest temperature. When the surface temperature is higher or lower than the active band, only the black color of the absorptive background is seen. The active band usually ranges from a few to several degrees Kelvin, yet with different combinations of thermochromic liquid crystals, a wide range of temperatures of 240 – 473 K can be measured [1,2]. In accordance with [3], the temperature range is 253 – 623 K, at the same time, with various kinds of liquid crystals, it is possible to detect changes in the temperature of the order of 0.1 K.

Being a precise and convenient method, thermography is widely applied. It provides a perfect means of quantitative temperature measurement, as it enables us to detect and observe a region which is warmer or cooler than the surroundings, without measuring the absolute temperature. The technique for temperature measurement on various surfaces and in fluids has been in use since the 1960s. The liquid crystal technique for the determination of temperature distribution on surfaces in heat transfer investigations is discussed, among others, in [4–14].

In spite of the advantages, the method has also a number of shortcomings, one of which is thermooptical hysteresis. The problem is that the color of the selective reflection at a certain temperature is different for heating and cooling [15]. Color differences are the more noticeable the bigger the amplitudes of changes in temperature. They are primarily calibration procedures, which have to directly accompany the measurement of the absolute temperature, that cause considerable difficulties.

Each measurement should be preceded by liquid crystals calibration in order to establish the relation between a color demonstrated on the surface and a corresponding temperature. Moreover, it is difficult to determine unambiguously standard colors, which is indispensable for repeatability of measurement results. It should be also remembered that the image of the temperature fields on liquid crystals covered surface changes with the observation angle and depends on the spectral composition of incident light. Hence there is a requirement that the same lighting conditions should be kept throughout all experiments.

1.2. Properties, forms of liquid crystals

As discusssed in [4], liquid crystals which react to temperature changes are called *thermotrophic*. In *thermotrophic* liquid crystals, due to the structure and the ordering degree, two mesophases can be differentiated: *smectic* and *nematic* [16,17]. These phases can be either *chiral* or *achiral*.

In nematic liquid crystals (Fig. 1a), elongated molecules belong to a big set of similar molecules, parallel to one another, or multi-molecular systems. This phase is far less ordered than smectic liquid crystals as nemetics do not show any other ordering, apart from the elements being parallel. Director "n" in Fig. 1a indicates the direction of molecule spatial orientation. In the smectic mesophase of liquid crystals (Fig. 1b), molecules parallel to one another are, additionally, arranged in such a way that molecule long axes are perpendicular to layer planes or inclined to them. The layers can move with respect to one another, which gives smectic liquid crystals the mechanical properties of a fluid.

The nematic phase can appear for those substances whose molecules are symmetrical with respect to their vertical axes or are not twisted with respect to those axes. Such nematic liquid crystals are called *achiral*. When elongated molecules of liquid crystal structures are not symmetrical with respect to their vertical axes or are twisted with respect to those axes, intramolecular forces make each molecule rotate slightly with respect to the neighboring one. As a result, the ordering direction of nematic liquid crystal, which is called *chiral nematic* or *cholesteric* takes the form of a helix with certain pitch, Fig. 2. The helical pitch (p) in chiral nematic liquid crystals is defined as distance at which "n" rotate by the angle of 360°. Optical properties seem to be the most important properties of liquid crystals. Owing to wave

interference, the most important property of some liquid crystals, it is possible to use them as temperature indicators. In accordance with Bragg's law, interference for a crystalline surface occurs when the crystal repetitive spatial pattern is "covered" by the half of the incident light wavelength. Then, the light is reflected in the same phase and amplified. In chiral nematic liquid crystals, interference takes place when the incident wavelength equals half of their helical pitch (Fig. 2). Consequently, when white light falls on such a liquid crystal, it will transmit all the waves apart from the one whose length equals its cholesteric helical pitch. The property is called *selective reflection.* As the only one wave is reflected and the remaining ones are transmitted, for the phenomenon to be clearly visible, it should be seen on the black absorbing background.
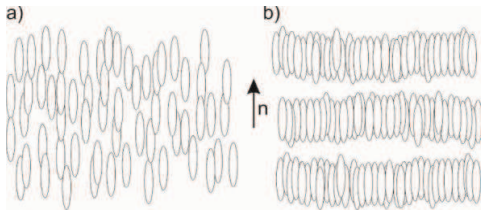

Fig. 1. Diagram of molecule arrangement in liquid crystals mesophase: a) nematic, b) smectic [16].
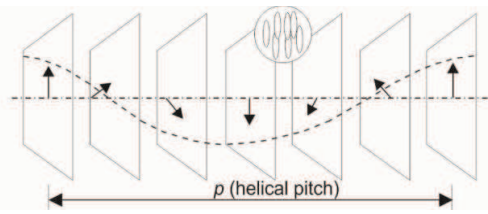
Fig. 2. Simplified diagram of the structure of chiral nematic liquid crystals.

Contamination, solvents, extreme temperatures and ultraviolet radiation lead to quick degradation of pure chiral nematic liquid crystals. The manufacturers of liquid crystal products developed different techniques to prolong the life of their products. Out of various available forms of liquid crystal indicators (non air-tight sealed layers, those pseudo-encapsulated or dispersed in film forming plastics), micro-capsules were selected for investigations. In the technology of their manufacture, the droplets of liquid crystals are covered with a continuous polymer film. Micro-encapsulating produces water suspension of discontinuous liquid crystal containing micro-capsules, on the average $10 \div 15$ μm in size. The best method of covering a surface is spraying it with this substance. Liquid crystal particles are protected as they are wrapped in a uniform film, at the same time, the film is the least harmful to the intensity and purity of selectively reflected light.

1.3. Color vs. temperature calibration of liquid crystal surface

Liquid crystals application to the detection of surface temperature must be preceded by color vs. temperature calibration of the liquid crystal surface. That has to be carried out under constant lighting conditions. Calibration should be repeated when a new batch of liquid crystals is used or when there are changes in any geometrical parameters of the image acquisition system. What should also be taken into account is that liquid crystals are affected by ageing.

Fig. 3 shows the set-up for liquid crystal calibration. It is composed of: a test section with a minichannel (#1), rotary pump (#2), heater with an electric heater element (#3), filters (#4), deaerator (#5) and autotransformer (#6). The test section with the minichannel is used in flow boiling heat transfer research; this issue has been discussed in Chapter 2, while the test section diagram has been shown in Fig. 4. The systems for data and color image acquisition and processing are shown in Fig. 5.

In the calibration process, water of the pre-set temperature is fed, in a closed cycle, to the minichannel, Fig. 3. Water is heated while it flows through the heater (#3), equipped with autotransformer (#6) for stepless power adjustment. The image of temperature distribution on

the surface is recorded by the following system (Fig. 5): investigated surface with thermochromic liquid crystals in the test section (#1), Canon G11 camera located opposite the surface (#2), lighting system consisting of fluorescent lamps emitting "cold white light"(#3a) and led bulbs (#3b) which are set at a specific angle to the surface. Water temperatures at the inlet and outlet to the minichannel are controlled with DaqBoard 2005 data acquisition station (#6) furnished with DASYLab software installed in a laptop (#7). On the other side of the minichannel, the Canon Eos 550D digital SLR camera (#4) with a special lighting system (#5) is used to observe two-phase flow structures investigated in heat transfer research.
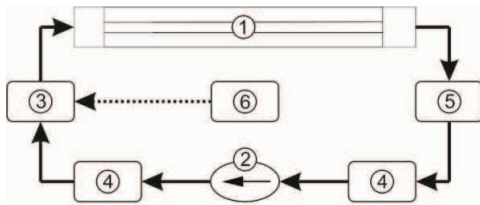

Fig. 3. Schematic diagram of the calibration loop: #1-test section, #2-rotary pump, #3-heater with an electric heater element, #4- filter, #5-deaerator, #6-autotransformer.
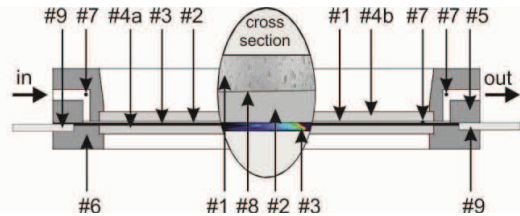

Fig. 4. The schematic diagrams of the test section: #1-minichannel, #2-heating foil, #3-liquid crystal layer, #4a,b-glass plate, #5-channel body, #6-front cover, #7-thermocouple, #8-enhanced side of the foil, #9-copper element.
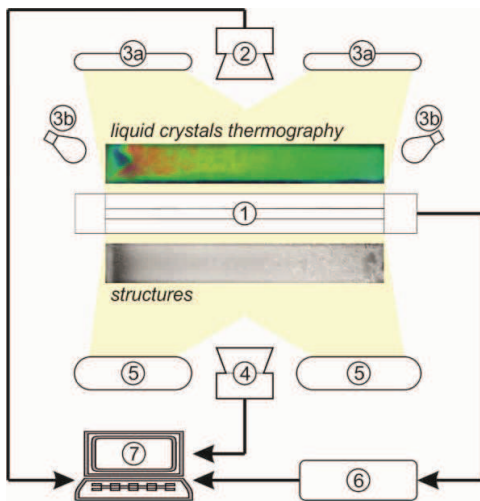

Fig. 5. The diagram of the experimental data and image acquisition system: #1-test section, #2-digital camera, #3-lighting system: #3a-fluorescent lamp, #3b-LED, #4-digital SLR camera, #5-high-voltage halogen reflectors, #6-data acquisition station, #7-laptop.
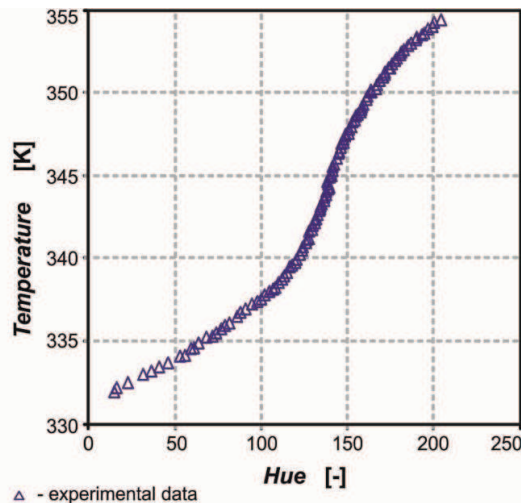

Fig. 6. Sample calibration curve [6].

In investigations, liquid crystals are used in the form of micro-capsules. The product of *Hallcrest Inc.*, (USA), model code R60C20W, of the width of 20 K of the active band was used. As mentioned, in the calibration process, for a pre-set temperature, a color image of the heating foil covered with a layer of liquid crystals is recorded. The mean value of RGB color components is determined for a pre-set surface, while the algorithm of image acquisition and processing was discussed below. Then, water is heated and a subsequent measurement is

taken for the next pre-set temperature. Experimental results of sample calibration in the form of a calibration curve are shown in Fig. 6.

1.4. Selected color models, algorithm of color image acquisition and processing

According to colorimetry theory, each color is composed of three basic colors, therefore, any random color can be specified by their linear combination. The system of color image acquisition based on three elementary colors: red, green and blue (RGB) was chosen. On the basis of color components RGB system, it is possible to construct, in the Cartesian coordinate system, a *chromaticity diagram*. Each point in the graph (Fig. 7a), i.e. each possible combination of the three components R, G, B will be located within an equilateral triangle. The vertexes of the triangle will be determined by the values of the basic color components. The triangle centre, which coincides with the beginning of the coordinate system, will be a point of white light, for which R, G and B take on the same value. In the *chromaticity diagram* in Fig. 7, it is assumed that the triangle side length equals $\sqrt{2}$.

Each point having coordinates *r, g, b* in the assumed system *XY* can be expressed with coordinates *x* and *y* in the following way [4]:

$$x = \sqrt{\frac{2}{3}}\left(r - \frac{g}{2} - \frac{b}{2}\right), \qquad y = \frac{g - b}{\sqrt{2}} \ . \tag{1}$$
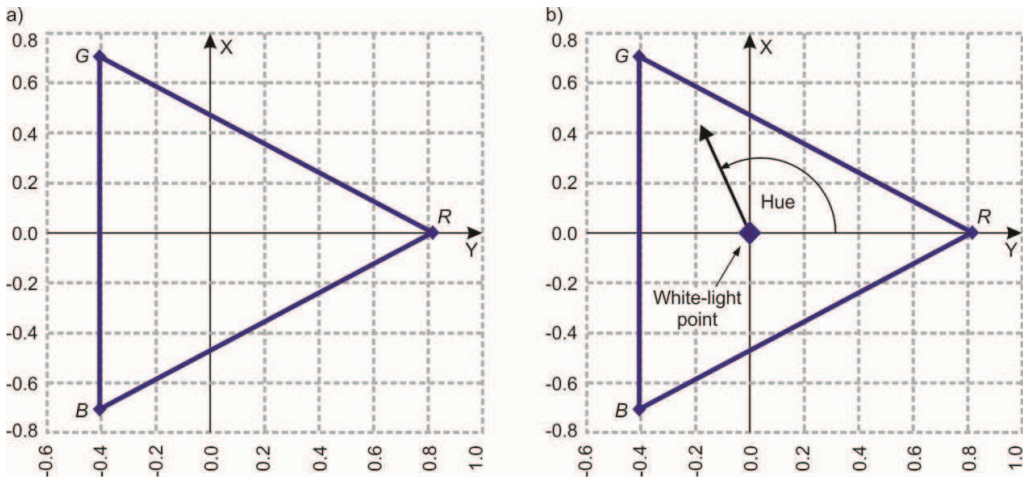

Fig. 7. System XY - chromaticity diagram illustrates color components dependence in the RGB system (a), polar coordinate system illustrates color components dependence in the HSI system (b) [4].

The RGB model, however, is not particularly convenient for interaction with a computer, that is, when the user has the possibility of directly specifying a necessary color. Simultaneously, the notation of each point in the form of a 3 x 1 matrix is not advantageous, either. Therefore other simplified color models were worked out: HSI, HSV, HLS and others. The HSI system will be discussed below; it allows, under certain specific conditions, the conversion of a three-component RGB signal into a single color matrix which is a scalar value – temperature will be ascribed a scalar colour dimension.

If the *chromaticity diagram*, based on rectangular coordinate system XY (Fig. 7a), is described in a polar coordinate system with the white light point as the system beginning, the position of a given point will be determined with polar coordinates which express the

dependence in accordance with the HSI system *(Hue, Saturation, Intensity)*. As the red color is described with the smallest light wavelength and the triangle vertex R is located on axis *X*, *hue* becomes an angle, which increases in a monotonic way with the increase in the wavelength, in accordance with light spectrum sequence, to violet *hue* of the biggest wavelength, Fig. 7b. *Hue* in the polar coordinate system represents the wavelength of the dominant color and is defined as an angle in the following way [4,5,7,18]:

$$hue = \arctan\left(\frac{y}{x}\right) = \arctan\left(\frac{\sqrt{3}(g-b)}{2r-g-b}\right) = \arctan\left(\frac{\sqrt{3}(G-B)}{2R-G-B}\right) \tag{2}$$

where: *R* – the content of red color component *G* – the content of green color component, *B* – the content of blue color component.

In the experiment of the color vs. temperature calibration of the liquid crystal covered surface, it is the color image that provides the basis for the determination of the two-dimensional surface temperature distribution. The system selected for the color image acquisition is based on three primary colors *R*, *G* and *B*. In order to process the registered color image, the HSI system is used. Custom-made software, developed in Delphi ver. 5.0 was used for acquisition and processing of the data on liquid crystal surface color vs. temperature calibration. The program records a color image corresponding to a pre-set temperature, in BMP format file and also RGB values for each image point in the text file. For each image point, *R*, *G* and *B* values are converted into *hue* and then averaged on the set surface. Calibration eventually yields the dependence *temperature = hue function*, which is called a *calibration curve*.

2. Liquid crystal thermography and of two-phase flow image analysis applied to investigations into boiling heat transfer in a minichannel

2.1. Experimental set-up

The test section (Fig. 4) with a minichannel of 1 mm depth, 40 mm width, 360 mm length, is the most important part of the experimental stand. The test section is set at various angles to the horizontal plane. The heating element for the working fluid (FC-72) flowing along the minichannel is a thin alloy foil (#2) stretched between the front cover (#6) and the channel body (#5). The foil is supplied with a direct current of controlled intensity. It is possible to observe both surfaces of the minichannel through two openings covered with glass plates. One plate (#4a) allows observing changes in the temperature of the foil surface as the side of the heating foil (between the foil and the glass) is covered with thermochromic liquid crystals paint (#3). Two-dimensional temperature field on the foil surface is determined by the color distribution on this surface thanks to liquid crystal thermography. The opposite surface of the minichannel (from the enhanced side of the heating foil) can be observed through the other glass plate (#4b), which helps recognize the vapor-liquid two-phase flow patterns. K-type thermocouples (#7) are installed at the inlet and outlet of the minichannel.

2.2. Liquid crystal color images of the heating foil

Fig. 8a shows subsequent images of the color distribution on the heating surface during the sample measurement batch at increasing (images from #1 to #6) and later decreasing (images from #7 to #10) heat flux supplied to the heating surface, obtained with liquid crystal thermography.

In Fig. 9, heating surface temperature dependences were derived from the images shown in Fig. 8a. They were constructed on the basis of the central part of the foil along the distance

from the minichannel, using the calibration curve from the calibration experiment. In the experiment, the application of liquid crystal thermography is essential because it enables observing the occurrence of the "boiling front". It is recognizable as the color sequence pattern, which indicates gradual color changes of the liquid crystals (in accordance with the spectrum sequence) and then sharp color changes of the liquid crystals (inversely to the spectrum sequence). Out-of-sensitivity-range temperatures are shown in black.
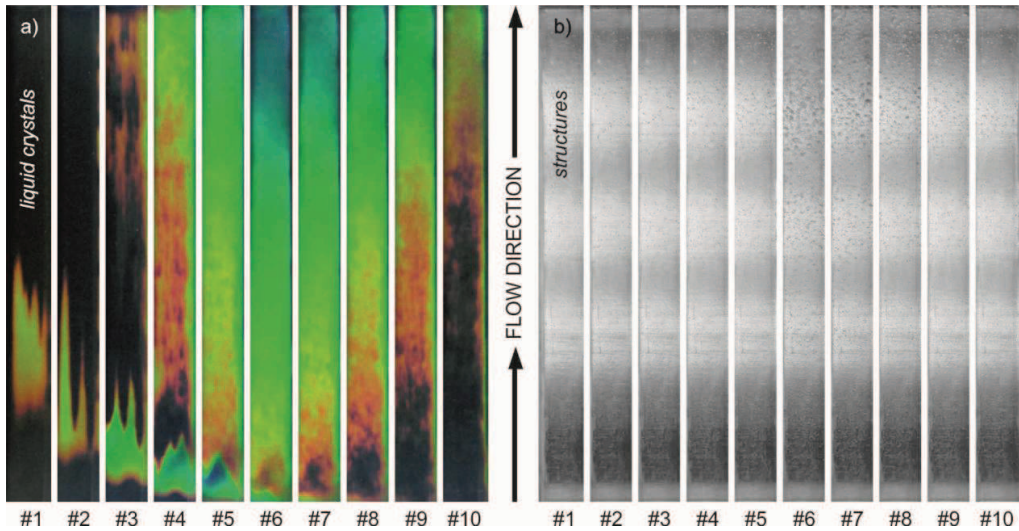

Fig. 8. Subsequent images of the color distribution on the heating surface during the sample measurement batch at increasing (images from #1 to #6) and later decreasing (images from #7 to #10) heat flux supplied to the foil (a), subsequent images of the two-phase flow structures during the sample measurement batch (b).

The boiling incipience is identified with the maximum value of the heating surface temperature in the "boiling front" image. A sharp temperature drop follows. The "boiling front" moves in the direction opposite to the direction of the liquid flow in the channel with increase of the heat flux supplied to the foil. The occurrence of nucleation hysteresis was discussed in [4-7]. Two-dimensional temperature distribution of the heating foil (Fig. 10c) for the preset area shown in Fig. 10b was constructed on the basis of the image selected from the batch (see Fig. 8a, setting #5) presented in Fig. 10a.
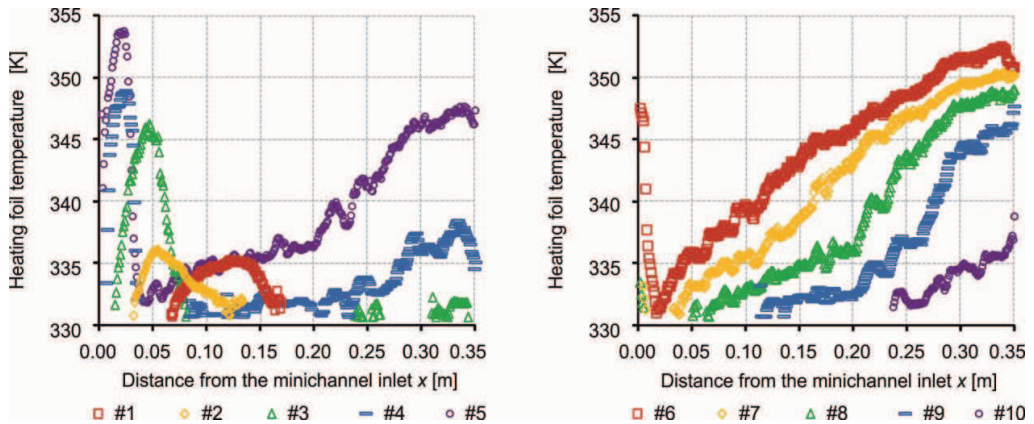

Fig. 9. Heating foil temperature vs. the distance from the minichannel inlet derived on the central part of the minichannel along its length, data attained from images shown in Fig. 8a.
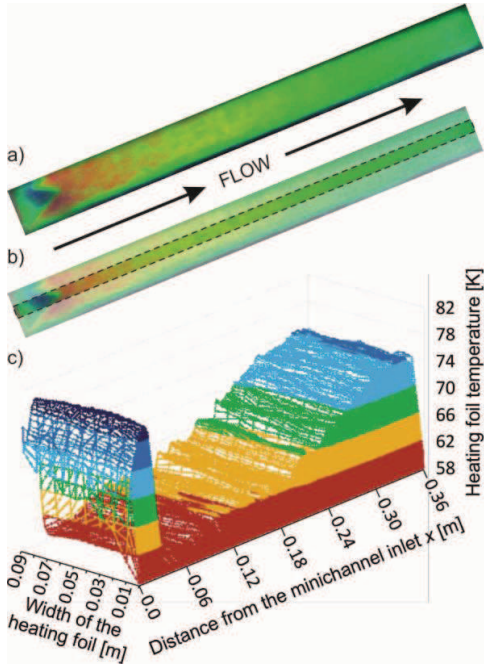
Fig. 10. Liquid crystal image, setting #5 (a); marked area for analysis of temperature distribution (b); two-dimensional temperature distribution of the heating foil (c).
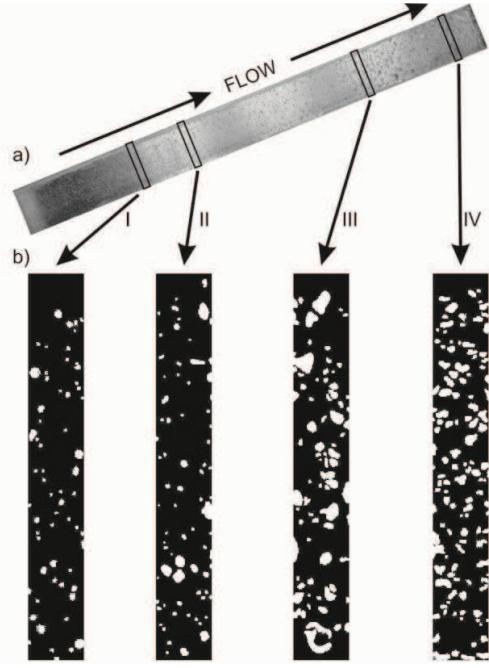
Fig. 11. Two-phase flow image, setting #7 (a), cross-sections of binarized two-phase flow structure image (b); white color refers to the vapor, and the black color represents the liquid.

2.3. Evaluation of the accuracy of heating foil temperature measurements with liquid crystal thermography

Error estimation is conducted in accordance with the principles of measurement accuracy analysis presented in [19]. Root-mean-square error is adopted as a measure of error quantity. Root-mean-square errors are computed as the roots of the sum of the second powers of the products of function partial derivatives, with respect to an external parameter occurring in a direct measurement, by the mean error of a given parameter measurement. The diagram with marked areas of error generation in the course of experiments is shown in Fig. 12.

The course of calculations used for the evaluation of the accuracy of heating foil temperature measurements with liquid crystal thermography is presented in [4,6]. Similarly to [4,6,18], it is assumed that the mean temperature error for the single point, determined on the basis of *hue* in the calibration experiment, amounts to:

$$\Delta T = \frac{1}{P}\sum_{i=1}^{P}\Delta T_p = \frac{1}{P}\sum_{i=1}^{P}\sqrt{\left(\frac{\partial T(hue_i)}{\partial hue_i}\cdot\Delta hue\right)^2 + \left(2\cdot SEE\right)^2 + \left(\Delta T_l\right)^2} \qquad (3)$$

where: i – measurement point; P – number of measurement points, T – temperature [K], Δhue – error in *hue* determination for a recorded and processed image; it is assumed that it equals double standard deviation, determined on the basis of the data for sample surface image in the calibration experiment; SEE – standard estimate of error in the fit of the calibration curve, determined with the use of the method of least squares, in accordance with the following formula:

$$SEE = \sqrt{\frac{\frac{1}{P}\sum_{i=1}^{P}\left(T(hue_i) - T_i\right)^2}{P - m - n}} \qquad (4)$$

at the same time: m – the order of polynomial approximating a calibration curve, $m=16$; n – derivative order, $n=1$; ΔT_l – absolute error in the measurement of liquid temperature at the minichannel inlet and outlet during calibration.
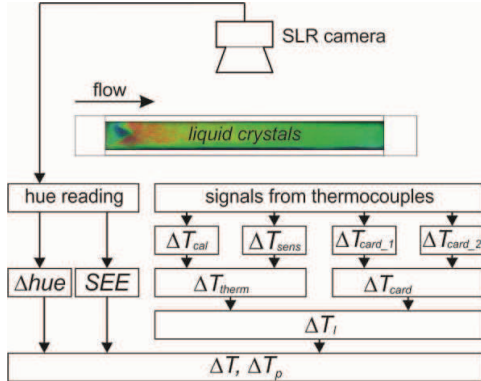

Fig. 12. Diagram with marked areas of error generation in the experimental data acquisition system.
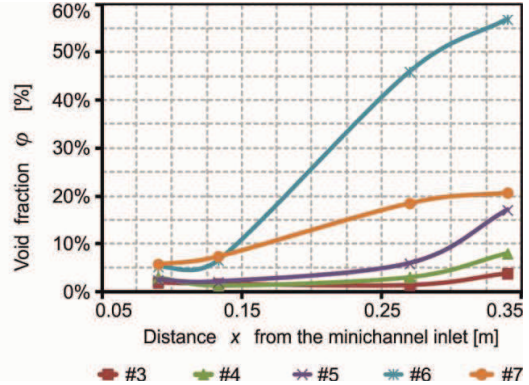

Fig. 13. Void fraction dependence along the minichannel length for selected cross sections for settings: #3, #4, #5, #6 and #7.

ΔT_l covers the errors resulting from signal processing by acquisition cards included in the measurement data acquisition station ΔT_{card} and the thermocouple sensor errors ΔT_{therm}.

The calculations of the absolute error in signal processing occur by appropriate cards of the *DaqLab 2005* measurement data acquisition station considering the errors in the thermocouple card DBK-83 with 14 inlet channels for thermocouples (ΔT_{card_1}), and in the station with 16-bit analogue-to-digital converter (ΔT_{card_2}). The calculations resulted in the determination that $\Delta T_{card\_1} = 64.54\mu V$ and $\Delta T_{card\_2} = 27.036$ μV, with the result $\Delta T_{card} = 69.974$ μV.

The absolute error ΔT_{therm} results from the error in thermocouple calibration ΔT_{cal} and the error in the measurement with thermocouple ΔT_{sens}. The following results were calculated: $\Delta T_{cal} = 6.582$ μV and $\Delta T_{sens} = 0.763$ μV.

Subsequent calculations led to $\Delta T_{therm} = 6.626$ μV and $\Delta T_l = 70.287$ μV. On the basis of thermocouple temperature measurement range (thermocouple type K, measurement range up to 1100°C), and in the temperature range of the thermocouple card (from 0 to 100 mV), 1K was obtained corresponding to 90.91μV. Therefore ΔT_l corresponds to the error in the temperature measurement $\Delta T_l = 0.77$ K.

Sample results of calculations in the error analysis for the conducted experiment are as follows: $P = 115$ calibration points: $\Delta hue = 1.45$; $SEE = 0.13$ and $\Delta T_l = 0.77$ K. After calculations made according to (3), $\Delta T = 0.86$ K was obtained [6].

2.4. *Monochrome images of flow structure analyses*

The analysis was based on the photographs of two-phase flow structures of heating foil taken by an SLR camera, obtained on the side coming into contact with fluid flowing in a minichannel, Fig. 8b.

After the two-phase flow had been analysed graphically and the image had been binarized, phase boundaries were determined in Corel software. The binarizing of the images helps determine the boundary between the liquid and the vapor. Methodology of the conversion of the greyscale image (8 bit) into monochrome image (1 bit) was presented in Table 1.

Table 1. Methodology of the conversion of greyscale image (8 bit) into monochrome image (1 bit)
- area of the bubble in the grid of 1x1 area (point);
- the blue lines delineate the boundary between phases;
- grey color – zones to be analyzed;
- green color – areas on the phase boundary with 50% or more of the area contained within the bubble;
- red color – areas on the phase boundary comprising below 50% of the area contained within the bubble;
- black color – ultimate area of the vapor taken for calculations, saved as 1 bit - monochrome image.
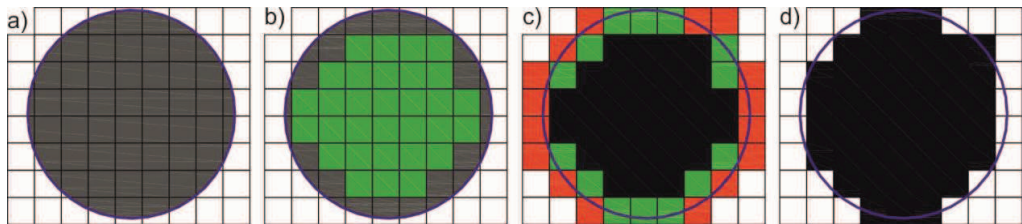
Then, the analysis of phase volumes was conducted in Techsystem Globe software. This software allowed the determination of areas of the two phases and/or percentage of the defined phase. Techsystem Globe software is a system for the stereological analysis of digital images used in quantitative analysis. Its principle of operation is similar to other image analysis applications such as popular Aphelion, NIS 3, NIS 4 (Nikon), Omnimet (Buehler), Visilog4, DP SOFT, CellSence Entry and CellSence Standard (Olympus). Nikon's NIS-Elements Advanced research software, version NIS 3 (updated to version 4.1) was used for comparison. There was a slight difference between these results and results obtained in Techsystem Globe software. It was found that the differences fall into the statistical error range and that these differences are brought about by the constraints implemented in mathematical morphological functions.

From the presented experimental data settings #3, #4, #5, #6 and #7 (see Fig. 8b) were selected for increasing heat fluxes supplied to the heating surface. Then, the void fractions were determined for 4 cross-sections (marked as I, II, III, IV) of each 5 x 40 mm image. The cross-sections were placed at the distance of 90 mm (I), 133 mm (II), 270 mm (III) and 336 (IV) from the inlets to the minichannels, as shown in the sample image – setting #7 presented in Fig. 11a. The enlarged binarized cross-sections of two-phase flow structure image adapted for analysis were presented in Fig. 11b.

The void fraction was determined according to the following formula [5−7]:

$$\varphi = \frac{V_v}{V_l + V_v} = \frac{A_v \cdot \delta_{ch}}{(A_l + A_v) \cdot \delta_{ch}} = \frac{A_v}{A_l + A_v} \tag{5}$$

where: V-volume, A-cross section area, δ-depth. In the notation, the subscripts referring to the liquid, the vapor and the minichannel are denoted with letters: l, v and ch, respectively.

Liquid and vapor cross-section areas were obtained from phase image analysis performed by means of Techsystems Globe software and with NIS-Elements Advanced Research software as the control. The results were presented as a void fraction dependence along the minichannel length in Fig. 13. As mentioned, the values of the void fraction obtained by the two computer programs were similar.

2.5. Measurement error of void fraction

As stated, after the two-phase flow image had been analysed graphically and the image had been binarized, phase boundaries were determined in Corel software. Due to the low depth of the minichannel (1 mm), the curvature of bubbles in the normal direction with respect to the surface of the heating foil (channel depth) was not taken into account. In evaluation, the absolute error of the void fraction was assumed to be equal to the area (point) comprising 0.0064 mm^2 [7], it results from the resolution of the image taken by a digital camera.

3. Conclusions

The technique of liquid crystal thermography provides an accurate, repeatable measurement of temperature distribution on the studied surface. For the technique to be effective, it is necessary to conduct calibration and maintain the same lighting conditions and distances between the components of the optical system, during both calibration and experiments. This measurement technique has been used for investigations into boiling heat transfer in cooling liquid flow through a minichannel. The technique helps detect two-dimensional temperature distribution on the foil forming the heating surface of the channel.

Because of the properties of liquid crystals, proper investigations have to be preceded by the calibration of the color of the surface with liquid crystal layer with respect to its corresponding temperature. Calibration must proceed under constant lighting conditions. The HSI system is used to convert a color image in RGB primaries obtained by the acquisition station. The system is of great convenience and it offers simplification in the processing of registered color image as, according to the system, it is possible to ascribe to a scalar quantity, i.e. temperature, a scalar, i.e. *hue*. The latter is read, instead of three components R, G and B, from the indications of liquid crystals sprayed over the heating surface.

The paper describes the method of visualisation of two-phase flow structures. The monochrome images of flow structures were analyzed to calculate the void fraction. The structure photos processed and binarized using Corel graphics software were used for the analysis of phase volumes developed in Techsystem Globe software (and with NIS-Elements Advanced Research software as the control). The estimations of measurement errors of the void fraction were relatively low. The applied method of visualisation is very interesting and research on this issue seems viable in terms of the acceptability of method accuracy. The investigation will continue in a follow-up research program.

References

[1] Collings, P.J. (1990). *Liquid crystals. Nature's delicate phase of matter.* Princeton: Princeton University Press.

[2] Kenning, D.B.R. (1992). Wall temperature patterns in nucleate boiling. *Int. J. Heat Mass Transf.*, 35(1), 73–86.

[3] Kasagi, N., Moffat, R.J., Hirata, M. (1989). *Liquid crystals. Handbook of flow visualization*. New York: Hemisphere.

[4] Piasecka, M., Poniewski, M.E. (2004). Liquid crystal thermography applied to investigations into heat transfer in minichanels, *Metrol. Meas. Syst.*, 11(3), 259–274.

[5] Piasecka, M. (2013). An application of enhanced heating surface with mini-reentrant cavities for flow boiling research in minichannels, *Heat Mass Transf.*, 49(2), 261-271.

[6] Piasecka, M., Maciejewska, B. (2012). The study of boiling heat transfer in vertically and horizontally oriented rectangular minichannels and the solution to the inverse heat transfer problem with the use of the Beck method and Trefftz functions. *Exp. Therm. Fluid Sc.*, 38, 19–32.

[7] Piasecka, M., Maciejewska, B. (2013). Enhanced heating surface application in a minichannel flow and use the FEM and Trefftz functions to the solution of inverse heat transfer problem, *Exp. Therm. Fluid Sc.*, 44, 23–33.

[8] Chan, T.L. (2001). Evaluation of viewing-angle effect on determination of local heat transfer coefficients on a curved surface using transient and heated-coating liquid-crystal methods. *Exp. Fluids*, 31, 447–456.

[9] Hay, J.L., Hollingsworth, D.K. (1996). A comparison of trichromic systems for use in the calibration of polymer-dispersed thermochromic liquid crystals. *Exp. Therm. Fluid Sc.*, 12(1), 1–12.

[10] Saniei, N. (2002). Liquid Crystals and Their Application in Heat Transfer Measurements, *Heat Transf. Eng.*, 23(4), 1–2.

[11] Yang, J.S., Hong, C.H., Young, M.B., (2007). Local heat transfer measurement from a pair of longitudinal vortices using a transient liquid crystal technique. *Exp. Heat Transf.*, 20(3), 197–212.

[12] Wang, Z., Ireland, P.T., Jones, T.V. (1995). An advanced method of processing liquid crystal video signals from transient heat transfer experiments. *Trans ASME J. Turbomachinery*, 117(1), 184–189.

[13] Ozer, A.B., Oncel, A.F., Hollingsworth, D.K., Witte, L.C. (2011). A method of concurrent thermographic-photographic visualization of flow boiling in a minichannel. *Exp. Therm. Fluid Sc.*, 35(8), 1522–1529.

[14] Konda Reddy, B., Balaji, C. (2012). Estimation of temperature dependent heat transfer coefficient in a vertical rectangular fin using liquid crystal thermography. *Int. J. Heat Mass Transf.*, 55(13-14), 3686–3693.

[15] Baughn, J.W., Anderson, M.R., Mayhew, J.E., Wolf, J.D. (1999). Hysteresis of thermochromic liquid crystal temperature measurement based on hue. *J. Heat Transf.*, 121(4), 1067–1072.

[16] Parsley, M. (1991). *The Hallcrest handbook of thermochromic liquid crystal technology*. Glenview, Illinois: Hallcrest Inc.

[17] deGennes, P.G. (1974). *The physics of liquid crystals.* Belfast: Oxford University Press.

[18] Hay, J.L., Hollingsworth, D.K. (1998). Calibration of micro-encapsulated liquid crystals using hue angle and a dimensionless temperature. *Exp. Therm. Fluid Sc.*, 18(3), 251–257.

[19] Holman, J.P. (1989). *Experimental methods for engineers.* New York: McGraw-Hill.